ASTRODYNAMICS TECHNIQUES FOR MISSIONS TOWARDS EARTH TRAILING OR LEADING HELIOCENTRIC ORBITS

Eric Joffre[(1)], *Valerio Moro*[(1)],
Florian Renk[(2)], *Waldemar Martens*[(2)]

(1) Airbus, Gunnels Wood Road, Stevenage SG1 2AS, UK
(2) ESA, Robert-Bosch-Straße 5, 64293 Darmstadt, Germany

ABSTRACT

Recent mission and system studies conducted for the European Space Agency have involved the design of transfers targeting Earth-trailing or Earth-leading heliocentric operational orbits, in a 1:1 resonance with Earth. Airbus is currently leading two such studies on behalf of the European Space Agency: the Lagrange (Space Weather) mission targeting the Sun-Earth L5 Lagrange Point, and the LISA (Laser Interferometer Space Antenna) constellation of three spacecraft, selected as the third large-class mission of ESA's Cosmic Vision Programme, and whose operational configuration consists in a heliocentric triangular cartwheel formation. As no ESA spacecraft has ever flown to these destinations, the presentation will focus on the mission analysis techniques applicable to this very special class of interplanetary missions, characterised by some unique features and challenges.

1. INTRODUCTION

The paper focuses on mission design techniques for missions towards Earth-Displaced Heliocentric Orbits (EDHO), either leading (Earth-Leading Heliocentric Orbits: ELHO) or trailing Earth (Earth-Tailing Heliocentric Orbits: ETHO).

A rare and very demonstrative example of such a mission is given by *NASA's Solar TErrestrial RElations Observatory* (STEREO) mission, whose mission design is described in [1]. The objective of the STEREO mission, successfully launched in 2006 by a Delta-II Launch Vehicle, was to provide coordinated and stereoscopic observations of the Sun and the interplanetary medium by using a two-spacecraft formation in heliocentric orbit, as shown in Figure 1. One spacecraft precedes the Earth in its orbit around the Sun and is named *Ahead* (STEREO-A); the other trails the Earth and is named *Behind* (STEREO-B). As evidenced by Figure 1, the STEREO spacecraft are on so-called *drift-away* heliocentric orbits: because of the heliocentric semi-major axis differential with respect to that of Earth (at 1 AU), they have a different orbital period around the Sun, and their heliocentric *mean motion* is either faster (for leading ELHOs) or slower (for trailing ETHOs) than Earth. Since their joint launch in 2006, STEREO-A and STEREO-B have been drifting away from Earth, they passed behind the Sun in 2015 and they are now following their course drifting back towards Earth, with a closest approach expected in 2023.

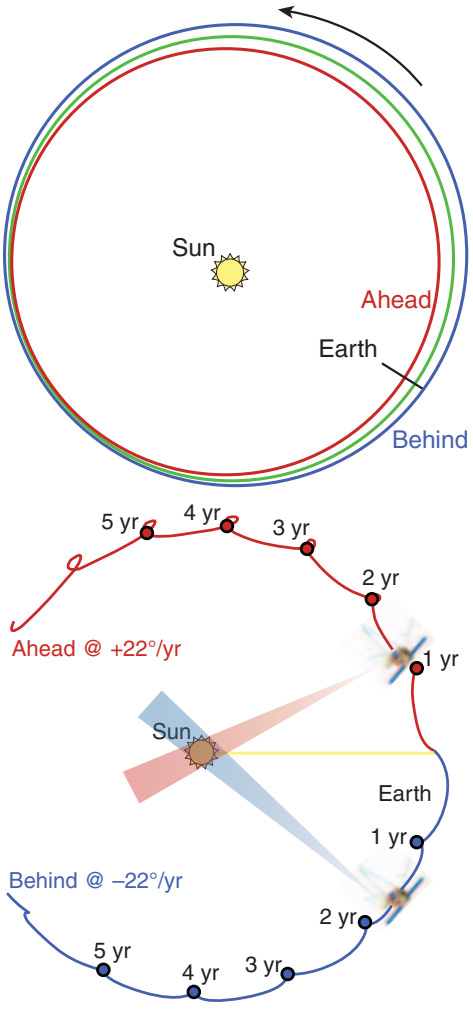

Fig. 1. Trajectory for STEREO-A and STEREO-B in inertial (top) and Sun-Earth rotating frame (bottom) (Credits: [1])

NASA's Spitzer Space Telescope is another example of a mission for which the operational orbit consists in an Earth-trailing drift-away orbit and whose mission design is presented in [2].

This paper will address a slightly different case, where instead of remaining on such drift-away orbits, the semi-major axis is corrected at the end of the transfer to match that of Earth, cancelling out the relative mean motion. As a result, the spacecraft reaches a heliocentric operational orbit in a 1:1 resonance with Earth. Such orbits for operational or science missions can present several benefits and provide candidate alternatives to more classical locations, such as the Sun-Earth Lagrange Point Orbits (LPO). In particular, they are characterised by near-constant distance and geometry with respect to the Sun and the Earth, thus potentially simplifying the spacecraft design, both for power generation (e.g. fixed Solar Array), communications (e.g. non-steerable Antenna), and thermal design (very stable and eclipse-free thermal environment). They are also characterised by a relatively stable orbit dynamics environment, thus requiring little or no orbit maintenance, as will be further described in the last section of the paper. Airbus is currently leading two system Phase A/B1 studies on missions for which such orbits are currently baselined: the *Lagrange Missions* and *LISA*, briefly introduced hereafter.

Lagrange Missions: ESA's Space Situational Awareness (SSA) programme, in particular with regards to Space Weather, is very important in enabling effective space operations and protecting ground-based infrastructures. Major Space Weather events, such as a *Carrington* level Coronal Mass Ejection (CME), pose a significant threat to both space and ground activities. The current satellites which monitor Space Weather are nearing the end of their life and need to be replaced to ensure continuity of solar observations. These current satellites primarily operate from a science perspective, with the focus on studying the Sun for scientific purposes. However, an operational monitoring capability is now required to ensure accurate and timely forecasts are consistently available to provide advanced warnings of solar activity which threatens Earth, so that appropriate mitigation actions can be taken. The Sun-Earth L5 (SEL5) and L1 (SEL1) Lagrange points are excellent locations for continuous monitoring of solar activity, with the measurements taken at these locations complementing each other. The L1 point enables in-situ measurements of the solar wind to be performed outside the influence of Earth's magnetosphere which provides information on solar wind conditions before they arrive at Earth. The L5 point, located at approximately 60 deg from the Sun-Earth line (trailing Earth), provides a view of a significant part of the Sun which is not yet visible from Earth and can therefore provide earlier warning of solar activity. A spacecraft at SEL5 can also monitor the entire space between the Sun and the Earth, allowing mid-course tracking of solar wind features and predictions of arrival times at Earth. The focus of the Lagrange Missions Phase A/B1 study is on an L5 mission, as schematically illustrated by Figure 2.

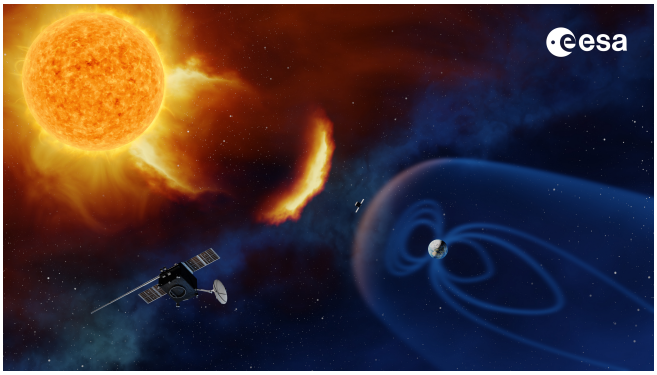

Fig. 2. Space Weather Lagrange Missions (Credits: ESA)

LISA: The main objective of the LISA mission is to observe gravitational waves emitted by a multitude of stellar, galactic and possibly cosmic sources, establishing the new field of gravitational wave astronomy. Recent breakthroughs have proven the feasibility of this ambitious goal: the first direct detection by the ground-based LIGO detector network of gravitational waves from a colliding binary black hole [3] has quickly been followed by more observations of various sources, including a neutron-star collision which also could be traced by other means of astronomy spanning the electromagnetic spectrum from gamma-rays to infra-red [4]. It turns out that this so-called multi-messenger astronomy is extremely effective in answering fundamental questions from physics and astronomy. Gravitational waves convey information on events otherwise hidden, as the universe is highly transparent for them. At the same time, the extreme stiffness of space-time gives rise to extreme technological challenges. Relative strains in the order of 10-20 have to be detected, limiting Earth-bound detectors to frequencies above 10 Hz, as seismic disturbances are omnipresent. Most sources of gravitational waves however are expected at frequencies between 10^{-4} Hz and 1 Hz, which is the measurement band addressed by space-based long-arm interferometers like LISA. LISA will consist of three identical spacecraft, launched together and deployed in an Earth-leading or Earth-trailing near-circular cartwheel formation. The three spacecraft are positioned in individual, initially fine-tuned heliocentric orbits. The triangle with a nominal apex-angle of 60 deg points toward the sun with a planar offset of ± 60 deg to the ecliptic and revolves around its centre once per year (Figure 3). All spacecraft are equipped with test masses which are in free-fall along the arms of the constellation. Gravitational waves cause picometer changes in the distances between these masses which are monitored interferometrically. To this end, there are three bi-directional laser links between the three spacecraft, spanning an arm length of approximately 2.5 million kilometres, which is required in order to provide

sufficient strain sensitivity at the lowest frequencies.

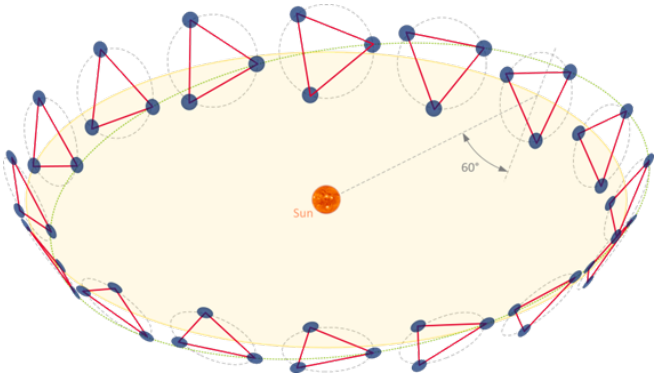

Fig. 3. LISA heliocentric cartwheel formation (Credits: ESA)

Outline of the paper: In this paper, the available injection and transfer strategies for the generic problem of a mission towards EDHOs (leading ELHOs or trailing ETHOs) will be reviewed: these include classical direct injection strategies, which will be thoroughly analysed first, but also low-energy escape options via the Sun-Earth L1 or L2 (SEL1/SEL2) points, as well as advanced strategies involving Gravity Assist Manoeuvres (GAM). The benefits and challenges of transfers augmented with Solar Electric Propulsion will be highlighted. A special attention will also be brought to the implications of the selected Launch Vehicle, in particular if characterised by a limited number of launch programs and range of available declinations (DLA), the resulting seasonal variation of the transfer problem and the impact of the launch windows definition.

The notation and acronyms that will be used throughout this paper are reported hereafter.

Notation

C3	Characteristic energy
ΔV	Delta-V (velocity increase)
ϵ	Axial tilt (or obliquity)
i	Inclination
ω	Argument of Perigee
Ω	Right Ascension of the Ascending Node (RAAN)
V_∞	Hyperbolic excess velocity

Acronyms

ACE	Advanced Composition Explorer
AoP	Argument of Perigee
ARM	Apogee Raising Manoeuvre
AU	Astronomical Unit (149597870700 m)
CME	Coronal Mass Ejection
CP	Chemical Propulsion
DLA	Declination of the Launch Asymptote
DSCOVR	Deep Space Climate Observatory
DSM	Deep Space Manoeuvre
EDHO	Earth Displaced Heliocentric Orbit
ELHO	Earth-Leading Heliocentric Orbit
EMB	Earth-Moon Barycentre
EME2000	Earth Mean Equator of epoch J2000
EOR	Electric Orbit Raising
ESSC	Earth-Sun-Spacecraft (angle)
ETHO	Earth-Trailing Heliocentric Orbit
GAM	Gravity Assist Manoeuvre
GSE	Geocentric Solar Ecliptic
GTO	Geostationary Transfer Orbit
HDOI	Heliocentric Displaced Orbit Insertion
HEO	High Elliptical Orbit
Isp	Specific Impulse
IAU	International Astronomical Union
JD	Julian Day
L5OI	L5 Orbit Insertion
LEO	Low Earth Orbit
LEOP	Launch and Early Orbit Phase
LGA	Lunar Gravity Assist
LISA	Laser Interferometer Space Antenna
LOI	Lissajous Orbit Insertion
LPF	LISA Pathfinder
LPO	Lagrange Point Orbit
LST	Local Solar Time
LV	Launch Vehicle
MEMB	Mean Earth-Moon Barycentre
MEDA	Mean Earth(-Moon Barycentre) Displacement Angle
NLP	Non-Linear Programming
OD	Orbit Determination
PO	Parking Orbit
RAAN	Right Ascension of the Ascending Node
SAA	Sun Aspect Angle
SEL1/2/5	Sun-Earth Lagrange Point L1/L2/L5
SEP	Solar Electric Propulsion
SOI	Sphere Of Influence
SSA	Space Situational Awareness
SSCE	Sun-Spacecraft-Earth (angle)
STEREO	Solar TErrestrial RElations Observatory
TCM	Transfer Correction Manoeuvre
TDB	Barycentric Dynamic Time
TLI	Trans-Lunar Injection
WSB	Weak Stability Boundary

2. REFERENCE FRAMES

As already illustrated in the previous section (Figure 1), transfer trajectories to EDHOs can be conveniently described in different coordinate systems. This section defines a few useful reference frames, as a prerequisite to the further description of the transfers, as well as the interpretation of some results. The next paragraphs successively introduce: the inertial *equatorial J2000* and *ecliptic J2000* reference frames, the true of epoch *Sun-Earth rotating frame*, and the *Sun-MEMB* (Mean Earth-Moon Barycentre) rotating frame.

2.1. Inertial Reference Frames

The *J2000 equatorial inertial reference frame*, or *EME2000* (Earth Mean Equator of epoch J2000) is the most commonly used inertial reference frame, and it is particularly relevant to describe geocentric[1] motion as well as injection conditions.

It is defined as follows:

- Z-axis = Z_{J2000}: Normal to the mean[2] equator of date at epoch 1 January 2000 at 12:00:00 TDB (Julian Day JD 2451545),
- X-axis = X_{J2000}: Line of Aries (or vernal equinox) direction, which is the intersection of the equatorial and the ecliptic planes at the same epoch.
- Y-axis: completing the right-handed trihedron.

The *ecliptic J2000 inertial reference frame* is obtained by a constant rotation from the aforementioned equatorial J2000 frame. The rotation angle from equatorial to ecliptic J2000 is of about $\epsilon = +23.44\,\mathrm{deg}$ (axial tilt), around the X_{J2000} axis.

2.2. Sun-Earth Rotating Frame

The Sun-Earth rotating frame is defined as follows:

- X-axis: pointing from Sun to Earth (true of epoch),
- Z-axis: towards the orbital momentum vector of the Sun-Earth system, perpendicular to the plane of the Earth's orbit around the Sun (ecliptic North of epoch),
- Y-axis: completing the right-handed trihedron.

The Sun-Earth rotating frame is commonly used to describe transfers to the Sun-Earth Lagrange Points, but it is also typically convenient for the visualisation of lighting conditions, such as the Sun Aspect Angle (SAA), the visualisation of eclipses from Earth during LEOP, as well as operational angles. An example of a (two-revolution) transfer to SEL5 is provided in Figure 4. It is a non-inertial frame, which is generally centred at Earth or at the Sun: a classical variant is the *Geocentric Solar Ecliptic* (GSE), for which the X-axis (pointing from Earth to Sun) and Y-axis are reversed.

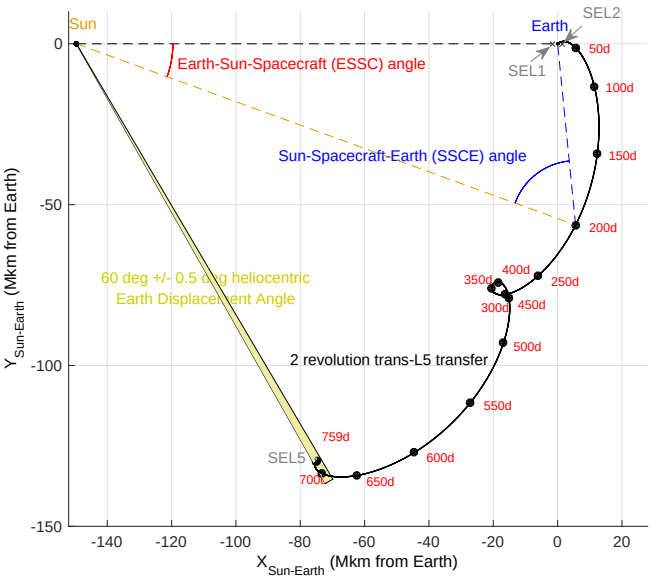

Fig. 4. Sample two revolution trans-SEL5 transfer and operational angles in Sun-Earth rotating frame

2.3. Sun-MEMB Rotating Frame

In order to describe some transfer trajectories, it is convenient to introduce a variant of the Sun-Earth Rotating frame, effectively getting rid of the Earth orbit's eccentricity around the Sun. This can be achieved by using instead the *Mean* Earth on its orbit around the Sun, and even better by considering the *Mean Earth-Moon Barycentre* (MEMB) to derive the rotating frame.

As the name suggests, the (true of epoch) *Earth-Moon Barycentre* (EMB) is obtained by considering, at each date, the barycentre of the Earth and the Moon. Given their respective masses, this fictitious point always lies under the Earth's surface, at a radius which varies roughly between 4,300 km and 5,000 km from the Earth's Centre of Mass. At each epoch, the *Mean* Earth-Moon Barycentre (MEMB) is derived by considering the osculating heliocentric orbit of this Earth-Moon Barycentre (EMB) and computing the corresponding mean orbit: with the same orbital plane (heliocentric inclination and RAAN), same period (semi-major axis), but on a perfectly circular orbit (eccentricity = 0), substituting the mean anomaly, derived from the true anomaly and eccentricity, to the true anomaly. The EMB and MEMB anomalies (heliocentric longitudes) thus coincide at perihelion and aphelion. The *Sun-MEMB rotating frame* can now be introduced in a similar way as for the Sun-Earth rotating frame, with:

[1] Both the equatorial and ecliptic J2000 *axes* define inertial frames, which can then be centred on any planetary body, typically Earth (geocentric), or the Sun (heliocentric) to serve as the basis for a coordinate system.

[2] precession model only (no nutation)

- X-axis: pointing from Sun to MEMB,
- Z axis: towards the orbital momentum vector of the Sun-MEMB system, perpendicular to the orbital plane of the MEMB's orbit around the Sun (effectively very close to the ecliptic North of epoch),
- Y-axis: completing the right-handed trihedron.

Figure 5 illustrates the respective trajectories of the (true) Earth and Moon in this newly defined frame, centred on MEMB, together with the position of the Earth for a sample set of 12 dates in the (arbitrary) year 2030.

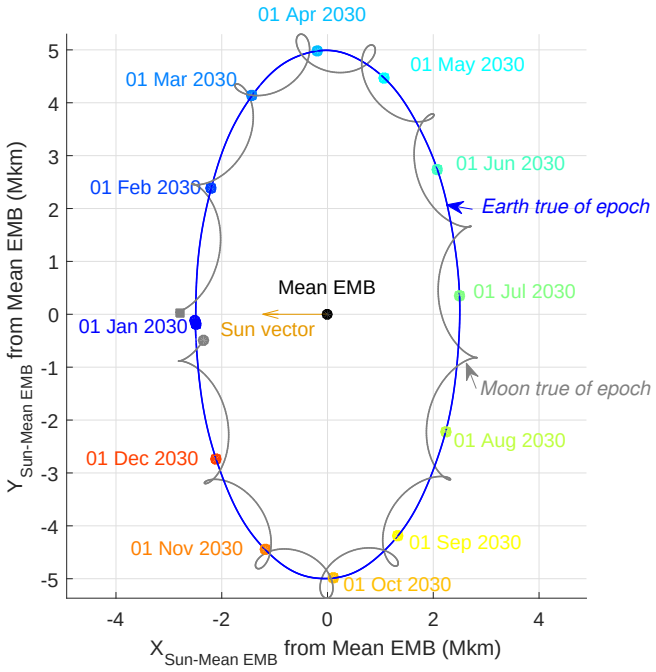

Fig. 5. Sun-Mean Earth-Moon Barycentre rotating frame and trajectories of the true of epoch Earth and Moon

As evidenced by this figure, the motion of the (true) Earth in this frame (blue) is that of a small ellipse, typical of a resonant formation flying-like relative trajectory[3] in the vicinity of a centre (MEMB) on a circular orbit around the central body (Sun), caused by a small eccentricity (about 0.0167 in this case). The out-of-plane motion, caused by the small inclination of the lunar orbit to the ecliptic, is insignificant. The motion of the Moon (grey) in this frame is more complex as it orbits the (true) Earth with an osculating orbital period of about 28 days. The distance of the (true) Earth to MEMB varies between 2.5 Mkm and 5 Mkm, and the Earth's relative velocity is maximum when it crosses the X axis at perihelion (prograde relative velocity, Y = 0, around January) and aphelion (retrograde relative velocity, Y = 0, around July) at about 1 km/s, and minimum when crossing the Y axis (X = 0, around April and October) at about 500 m/s.

This frame is more appropriate to describe heliocentric trailing/leading orbits at 1 AU than the Sun-(true) Earth rotating frame. Indeed, the motion of a spacecraft on a heliocentric and perfectly circular orbit trailing (respectively leading) Earth would exhibit a periodic motion that is indirectly caused by the Earth orbit's eccentricity, if seen from Earth in the Sun-Earth rotating (or GSE) frame, while on the other hand, the position of such a spacecraft is fixed in the Sun-MEMB rotating frame. Examples will be provided later on, see for instance Figure 14. Another advantage is that the departure (launch) date is directly visible on trajectory plots as the motion of the Earth is described by Figure 5.

3. PROBLEM STATEMENT

In the Sun-MEMB rotating frame defined in the previous section, the problem of the transfer optimisation to the target EDHO can be described as departing from an initial "planar cartwheel" (Earth) to rendezvous with a fixed point in the Sun-MEMB rotating frame, lying at a different heliocentric inertial longitude than the Earth. This heliocentric inertial longitude differential with respect to the Earth-Moon Barycentre will be referred to as the *Mean Earth Displacement Angle* (MEDA) in the rest of the paper.

While the actual target orbit for a given mission is likely to be compatible with (or even to require[4]) some heliocentric inclination (originating a periodic motion out of the ecliptic) and eccentricity (causing an in-plane periodic motion around the mean fictitious centre), the paper will address the case where the target position lies at exactly 1 AU from the Sun without any residual eccentricity or inclination.

4. SOLUTION SPACE ANALYSIS FOR DIRECT INJECTION

In this section, the direct injection scenario is investigated. The first paragraph provides a simplified analysis where the spacecraft would depart from the fictitious Mean Earth-Moon Barycentre (MEMB) on a circular heliocentric orbit at 1 AU, to reach a target position with a non-zero Mean Earth Displacement Angle (MEDA). Then, the impacts of the injection from an actual Earth-bound orbit are analysed, without any constraint on the Declination of the Launch Asymptote (DLA), assuming the capability from the Launch Vehicle to inject the spacecraft in the ecliptic, before briefly addressing the consequences of a constrained near equatorial launch.

4.1. Preliminary Analysis with Departure from MEMB

The assumptions for this analysis are the following:

[3] in-plane *flyaround* or *cartwheel* with ellipse semi-major axis twice the value of the semi-minor axis.

[4] such as LISA for which the operational science orbit mandates a very specific relationship between the orbit's eccentricity and inclination.

- The dynamics is modelled by the simple Keplerian motion of a Sun-centred two-body problem, not accounting for any perturbation and in particular the Earth's gravity.
- The initial (MEMB) and final (EDHO) orbits are both heliocentric circular (at 1 AU) and coplanar (ecliptic).
- The initial velocity (inertial, before the departure Delta-V), is that of the MEMB under the above assumptions.
- The final manoeuvre (arrival Delta-V) is cancelling the velocity differential between the spacecraft and the target. Only ballistic transfers are sought in this paragraph, with no Deep Space Manoeuvre (DSM).

As a result of the above assumptions, the dynamical system, and therefore the transfer problem, are time-invariant: the properties of the solutions do not depend on the departure date but only on the transfer duration. The problem is also symmetric and solutions are characterised by an initial Delta-V at departure that is equal to the final Delta-V upon reaching the EDHO to stop at the required MEDA. Figure 6 shows the Delta-V curves (for either departure or arrival, Y-axis) as a function of the transfer duration (X-axis) and MEDA target (different curves, from ± 10 deg to ± 45 deg orbits).

The analysis of the solution space for this simplified problem shows that theoretical solutions exist for *all* transfer durations. For multiple revolution transfers, the Lambert transfer problem has two distinct solutions, providing that the transfer duration is greater than a minimum value. On Figure 6, when several transfer solutions exist, only solutions with minimum heliocentric eccentricity are shown, which also corresponding to the minimum Delta-V. The apparent singularities in the Delta-V curve correspond to the switching from one type of solution to the other. For a same angular displacement (MEDA absolute value), leading orbits are more expensive to reach than trailing orbits, since lowering the perihelion requires more Delta-V than raising the aphelion by the same amount. On the other hand, transfers are shorter as the transfer orbits correspond to lower orbital periods (semi-major axis below 1 AU).

Figure 6 also shows the relatively linear behaviour of the transfer Delta-V and of the transfer duration a function of the target MEDA, within each local minimum region. The set of local minima around 350/400 days corresponds to single revolution transfers, while the set of local minima around 700/750 days correspond to two-revolution transfers, typically characterised by an additional year of transfer, and a reduction by about half of the (departure and insertion) Delta-V. Figure 7 illustrates optimal trajectories towards ETHOs for the single revolution cases, in the Sun-MEMB rotating frame.

As observed on Figure 7, optimal trajectories in this preliminary simplified model correspond to basic Hohmann transfers: transfers to Earth-trailing (resp. Earth-leading)

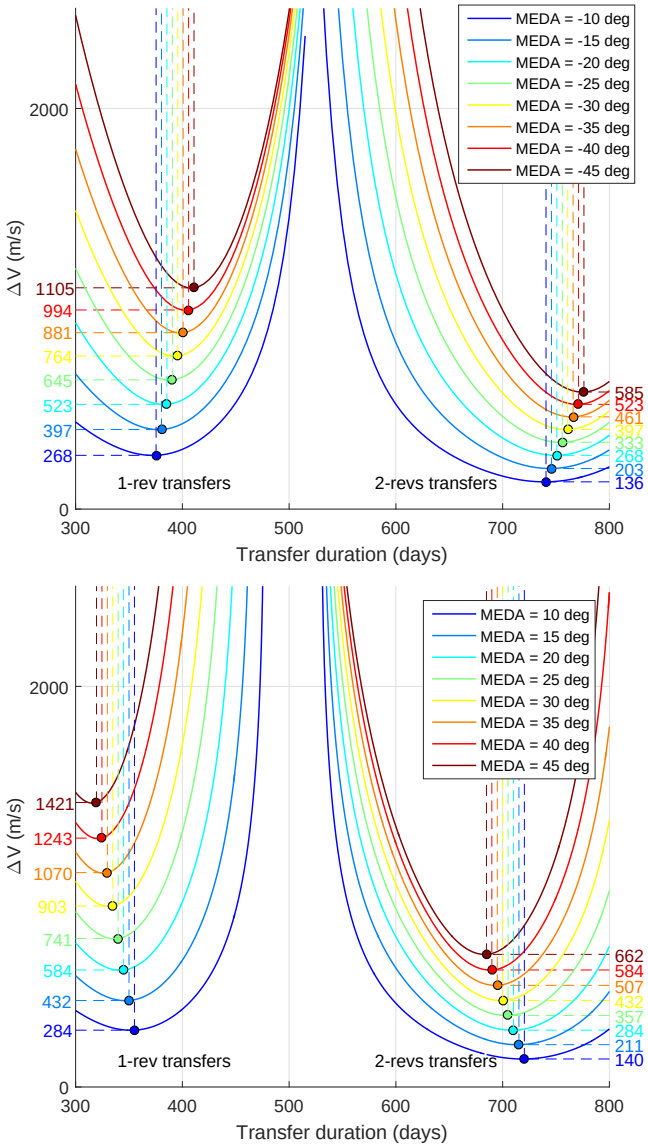

Fig. 6. Transfers towards ETHOs (top) and ELHOs (bottom): Delta-V as a function of the transfer duration and MEDA

orbits depart at their heliocentric perihelion (resp. aphelion), and reach the ETHO (resp. ELHO) when at perihelion (resp. aphelion) again, after one (single revolution) or more (multiple revolution) orbital periods. For these solutions, the departure and arrival manoeuvres are performed tangentially, with a departure Delta-V equal to the arrival Delta-V.

4.2. Ballistic opportunity maps and limitations

In this section, the impacts of the Earth orbit's eccentricity around the Sun on the transfer solution space are highlighted. The analysis of the previous paragraph is repeated, but instead of departing from the fictitious MEMB, opportunities departing Earth (true of epoch) are sought. Because of the eccentric

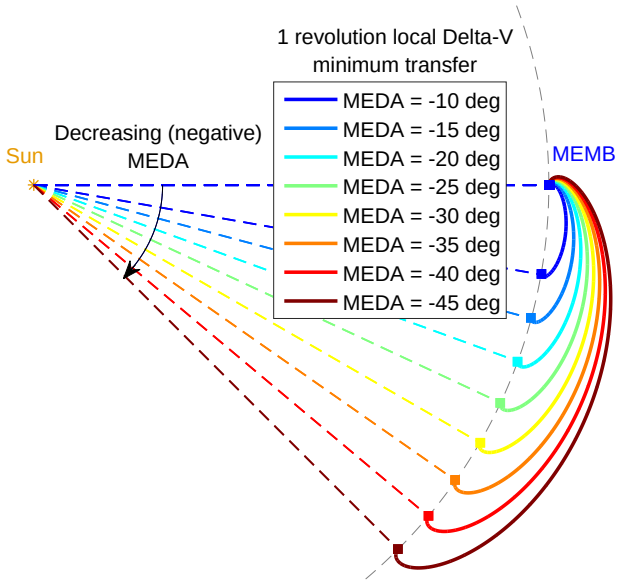

Fig. 7. Optimal single revolution transfers to various MEDA targets on the 1 AU ring (Sun-MEMB rotating frame)

orbit of the Earth, the problem is no longer time-invariant and symmetric (in departure/arrival). The assumptions of a heliocentric Keplerian motion and ballistic DSM-free transfer are maintained, and *pork chop* opportunity maps are generated, varying the departure date (within the sample year 2030) and transfer duration. Results are shown on Figure 8 (durations close to previous single revolution optimum) and Figure 9 (durations close to previous two-revolution optimum), for an example of ETHO target at MEDA = -30 deg. Only Delta-V below 2 km/s are shown on the contour plots.

It can be observed from the opportunity maps that the problem is no longer time-invariant, but 1 year periodic as expected. A second order variation, characterised by a short-term (about one month) indirect effect of the Moon is also visible on the departure Delta-V maps. A seasonal variation is noticeable, with low departure Delta-V periods (e.g. October to April) corresponding to high arrival Delta-V periods for transfers to ETHOs, and the situation is reversed for transfers to ELHOs. This result can again be easily interpreted by the fact that during this period, the Earth lies in the inner part of its orbit around the Sun, closer to perihelion (see Figure 5). Since raising the semi-major axis (as required by a transfer towards an ETHO) is more efficient when performed at perihelion, the injection Delta-V is lower from October to April. On the other hand, these solutions are therefore also those maximizing the heliocentric transfer orbit's eccentricity (low perihelion and high aphelion), which accounts for the significantly higher Heliocentric Displaced Orbit Insertion (HDOI) Delta-V upon reaching the target (circular) ETHO.

This inherent property of the transfer problem is highly

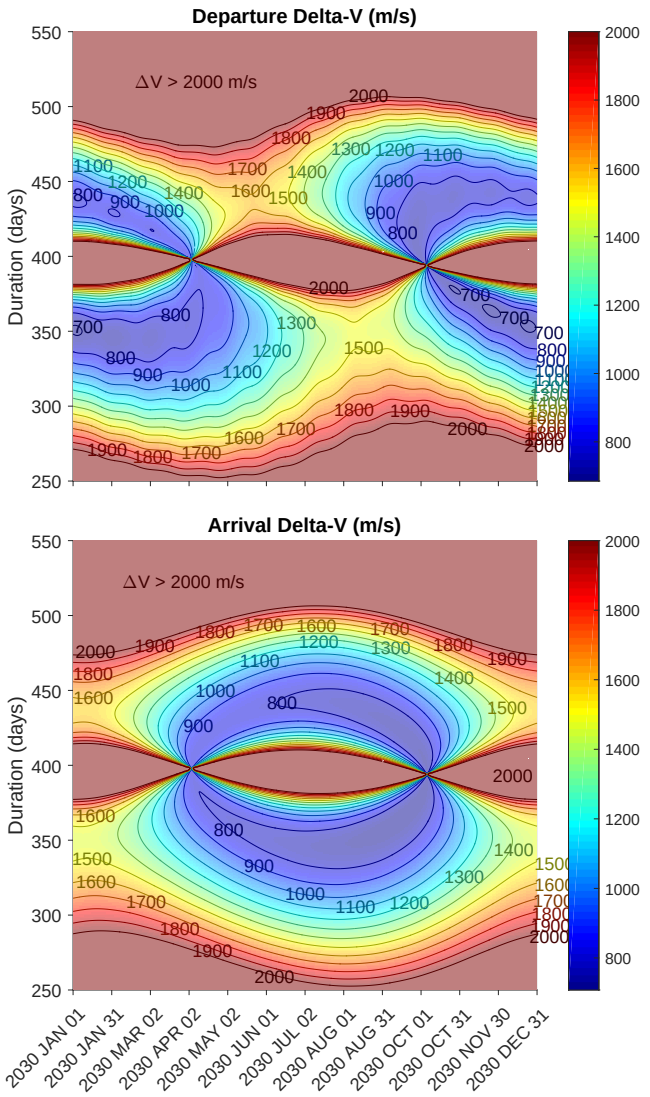

Fig. 8. Heliocentric Keplerian single revolution ballistic opportunity map towards ETHO (-30 deg)

undesirable from a mission and spacecraft design point of view: using such solutions would indeed require a high number of launcher programs (departure C3) as a function of the launch date, and also require a very different amount of propellant depending on the launch month, in case a year-round launch capability is required (no launch window restriction).

Another essential point to be observed on these maps is that singularities occur near the previously identified durations, with a very steep increase of the departure and arrival Delta-V. Indeed, the previously identified local minima solutions corresponded to Hohmann-like transfers, as described in the previous paragraph, completing an integer number of full heliocentric revolutions. Such solutions cannot be available departing from an eccentric heliocentric orbit, such as

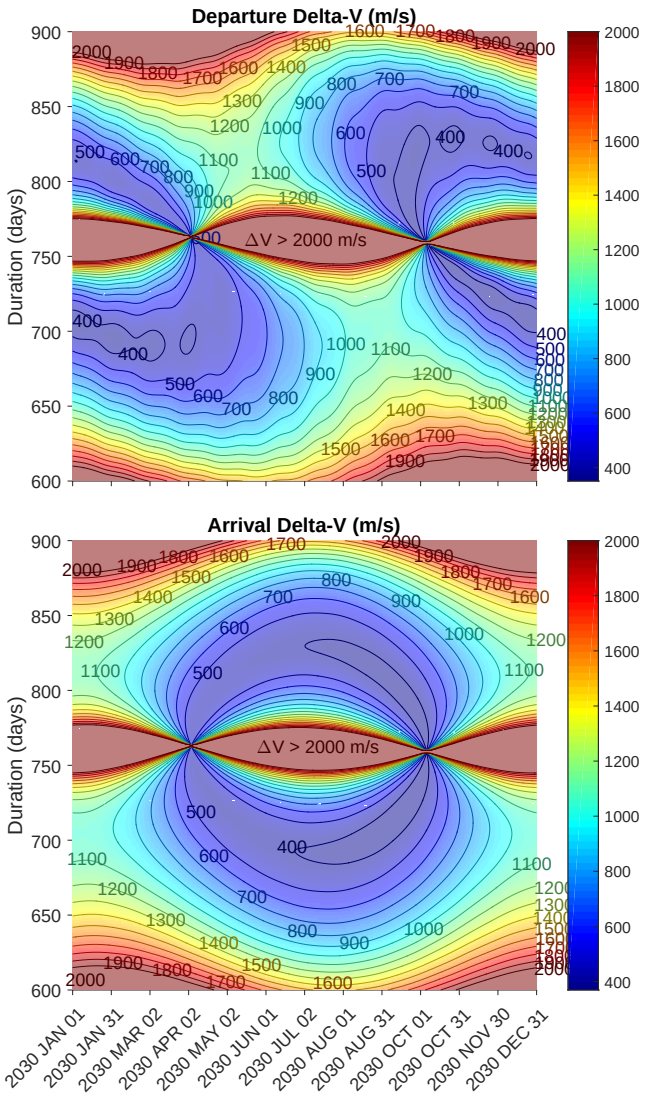

Fig. 9. Heliocentric Keplerian two-revolution ballistic Keplerian opportunity map towards ETHO (-30 deg)

the one of the Earth, since - except for two very specific dates within the year where the Earth is exactly at 1 AU (around 1st October and 1st April) - the departure and arrival positions have different heliocentric radii. We will see in the next section that the introduction of a (single) Deep Space Manoeuvre (DSM) during the interplanetary cruise will largely improve the situation for these two identified issues.

4.3. Transfer Opportunities with DSM and Injection into the Ecliptic

The objective of this section is to derive EDHO transfer results in conditions that could be representative of an actual mission scenario. The transfer analysis is therefore revisited with the following major updates:

- Actual injection conditions are considered, departing Earth from a given escape (hyperbolic orbit), and accounting for Earth's gravity. The injection state is characterised by the geocentric osculating orbital elements at perigee, with respect to the equatorial J2000 reference frame.[5]
- A single value of the hyperbolic excess velocity (escape V-infinity) is considered throughout the year: the Delta-V value from the preliminary analysis departing from MEMB is used in the following results.
- A (single) Deep Space Manoeuvre (DSM) is permitted during the heliocentric cruise towards the target EDHO.
- A minimum duration of 30 days between DSM and Heliocentric Displaced Orbit Insertion (HDOI) is enforced as an optimisation constraint, in order to allow for Orbit Determination (OD) and Transfer Correction Manoeuvres (TCM) prior to insertion.

In this section, a launch directly into the ecliptic plane (by means of inclination i and RAAN Ω tuning) is assumed, as this is naturally the optimum injection orbital plane to reach the target (ecliptic) orbit. This assumption will be discussed in the next section. Such a scenario could typically be the one where a low-inclined circular Parking Orbit (PO) is used before a re-ignition of the upper stage of the Launch Vehicle at an optimal time, thus setting the value of the Argument of Perigee (AoP, ω) of the escape orbit. A fixed perigee altitude of 250 km is considered.

In this new problem, many degrees of freedom are available as optimisation parameters (decision variables), including the injection AoP, the date, direction and magnitude of both the DSM and the HDOI manoeuvres. The introduction of a DSM drastically alters the structure of the solution space previously described. Figure 10 shows a sample opportunity map, corresponding to a launch on 1 January 2030, for a transfer towards a target ETHO with MEDA = -30 deg (escape V-infinity = 764 m/s, looking for single revolution-like transfers). The X-axis represents the AoP (ω), the Y-axis the total transfer duration (from injection until HDOI). For each point of the domain (ω, duration), the date, direction and magnitude of the DSM are optimised, and the properties of the HDOI manoeuvre are derived to ensure rendezvous with the target ETHO for the required transfer duration. The contour plots represent the resulting sum of the DSM and HDOI Delta-V. Similar opportunity maps are provided on Figure 11 for May and September launch dates to illustrate the variety of possible situations.

The analysis of Figure 10 gives an indication of the challenges posed to an NLP solver presented with such an optimisation problem: multiple local minima are observed, as

[5]The perigee could well be a fictitious perigee as the Launch Vehicle would typically insert the spacecraft on an orbit after perigee.

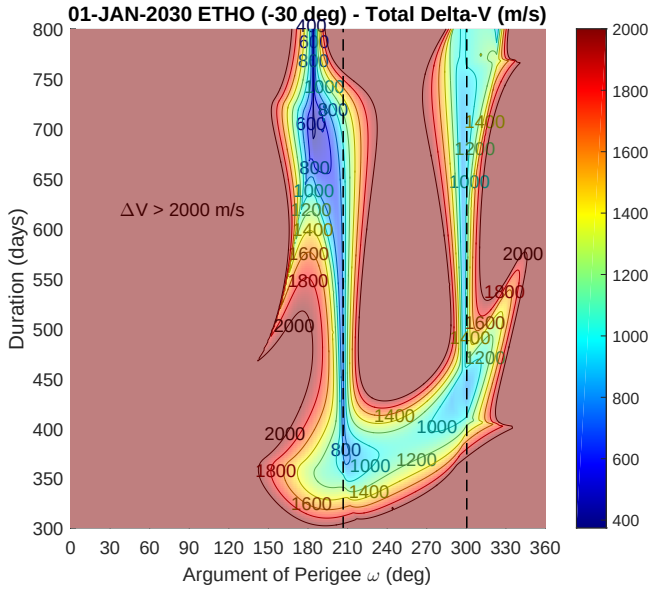

Fig. 10. Opportunity map for January launch towards -30 deg ETHO with optimised DSM

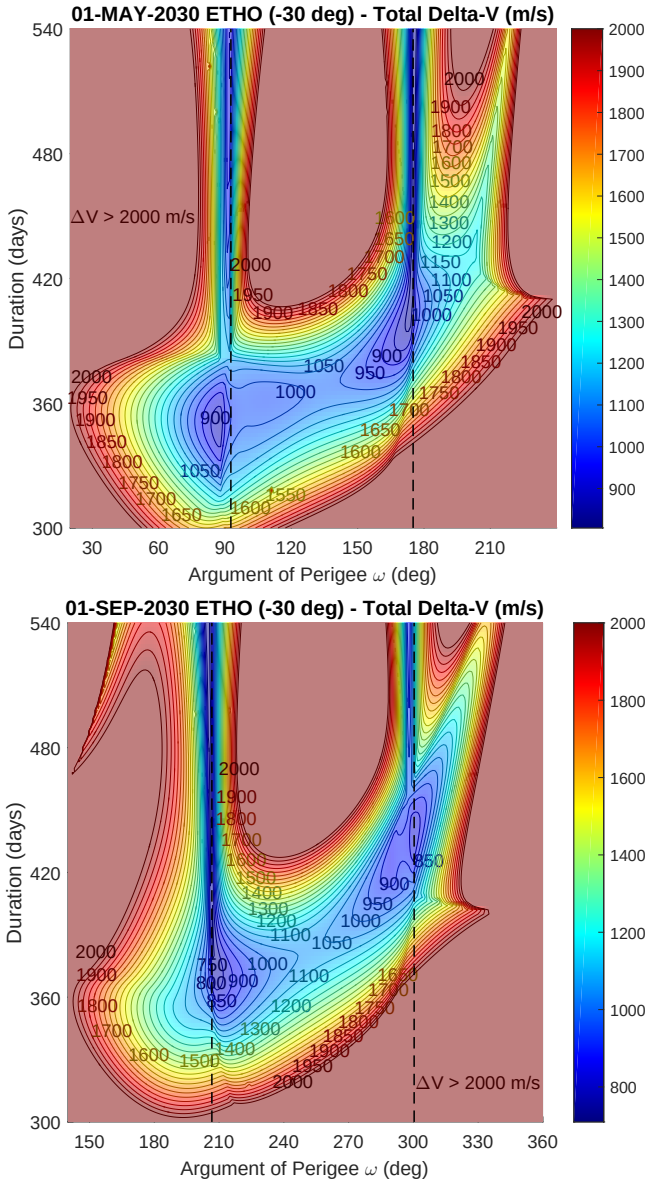

Fig. 11. Opportunity map for May (top) and September (bottom) launch towards -30 deg ETHO with optimised DSM

well as very narrow strips of low Delta-V regions, for which the sensitivity to the transfer duration is low (shallow Delta-V along the Y-axis), while the sensitivity to the AoP is very high, with very steep Delta-V increase when moving away (along the X-axis) from the minimum. Good initial guesses are therefore needed for some decision variables to ensure convergence towards a global optimum. Regarding the AoP, one can be derived by solving for each date the values that correspond to a heliocentric semi-major axis, evaluated as the spacecraft leaves Earth's Sphere of Influence (SOI), equal to the value that would be required to complete a full Keplerian revolution around the Sun before reaching the target MEDA, that is to say by looking for quasi-Hohmann transfers. Two such AoP values are generally admissible (depending on the launch V-infinity), and represented on Figure 10 and 11 by the vertical black dashed lines.

An interesting property of the new solution space is that there is no longer a clear distinction between the single and the two (or more) revolution transfers, but instead a continuum of low Delta-V regions in the vicinity of the two initial guesses for the AoP. It is therefore required to constrain the maximum acceptable transfer duration to formulate the optimisation problem: a maximum duration of 540 days is considered in the rest of the section.

Figure 12 illustrates on the same plot the corresponding optimal transfers for the January, May and September launches, in the Sun-MEMB rotating frame. One can see on these trajectories that the solutions of the short type (like January) are typically characterised by a relatively very small DSM and a very large insertion manoeuvre, resembling solutions of the preliminary Keplerian analysis. Conversely, the long type (like May and September) are typically characterised by a very small (HDOI) insertion manoeuvre and a large DSM, already relatively "close" to the target EDHO as seen from the Sun-MEMB rotating frame. In fact, the DSM is in that case an insertion manoeuvre into a slowly drifting orbit towards the final EDHO. It also appears on the three trajectory examples that the large manoeuvres performed close to / at the target ETHO are retrograde manoeuvres performed almost exactly along the anti-(absolute) velocity vector, which is indeed a characteristic of optimal transfer solutions. A synthesis of the results for Delta-V minimum transfers (under

the constraint of a maximum transfer duration of 540 days) is provided in Table 1. The Delta-V is the sum of the DSM and of the insertion manoeuvre, and the transfer duration is the total duration from injection (perigee) until insertion.

Table 1. Transfer opportunities with DSM and injection into the ecliptic - Results for transfers to -30 deg ETHO for each month (duration lower than 540 days)

Injection date	Delta-V (m/s)	Duration (days)	AoP (deg)
01-Jan-2030	945.95	369.50	319.50
01-Feb-2030	981.98	411.00	93.50
01-Mar-2030	920.59	406.00	119.50
01-Apr-2030	834.03	400.00	146.00
01-May-2030	801.06	540.00	175.75
01-Jun-2030	779.33	351.50	121.5
01-Jul-2030	746.96	540.00	147.80
01-Aug-2030	720.46	540.00	175.80
01-Sep-2030	706.83	540.00	204.75
01-Oct-2030	710.10	540.00	234.25
01-Nov-2030	785.67	378.00	262.00
01-Dec-2030	874.55	375.00	289.50

The results show a significant seasonal variation, already observed in the previous analyses, with low Delta-V transfers to trailing orbits only available for half the year. The seasonal variation of the Delta-V curve as a function of the launch date would be mirrored for transfers towards Earth-leading orbits.

4.4. Direct Ascent from Earth with Constrained DLA

This section is relevant to scenarios where the departure conditions (injection) are constrained in the Declination of the Launch Asymptote (DLA, measured in the equatorial inertial frame). This is especially applicable to direct ascent launches with Ariane from Kourou, as the optimal performance for this future Launch Vehicle is likely to be for a GTO-like injection, characterised by an inclination of about 6 deg and an argument of perigee of 178 deg, therefore placing the line of apses close to the equatorial plane. In this case, the value of the Right Ascension of the Ascending Node (RAAN, Ω) of the escape orbit is defined by the injection time. The analysis is very similar to that of the previous section, effectively replacing the Argument of Perigee as a free parameter by the RAAN, so only the conclusions are outlined. As a Delta-V optimal transfer trajectory to the target EDHO requires a specific orientation of the line of apses with respect to the Sun line, a limitation on the available injection orbit's inclination and Argument of Perigee (in the inertial equatorial frame) caused by a limitation by the Launch Vehicle will result in a seasonal variation of the transfer orbit's heliocentric inclination. This extra out-of-plane motion needs to be corrected (during transfer and) upon insertion into the target EDHO.

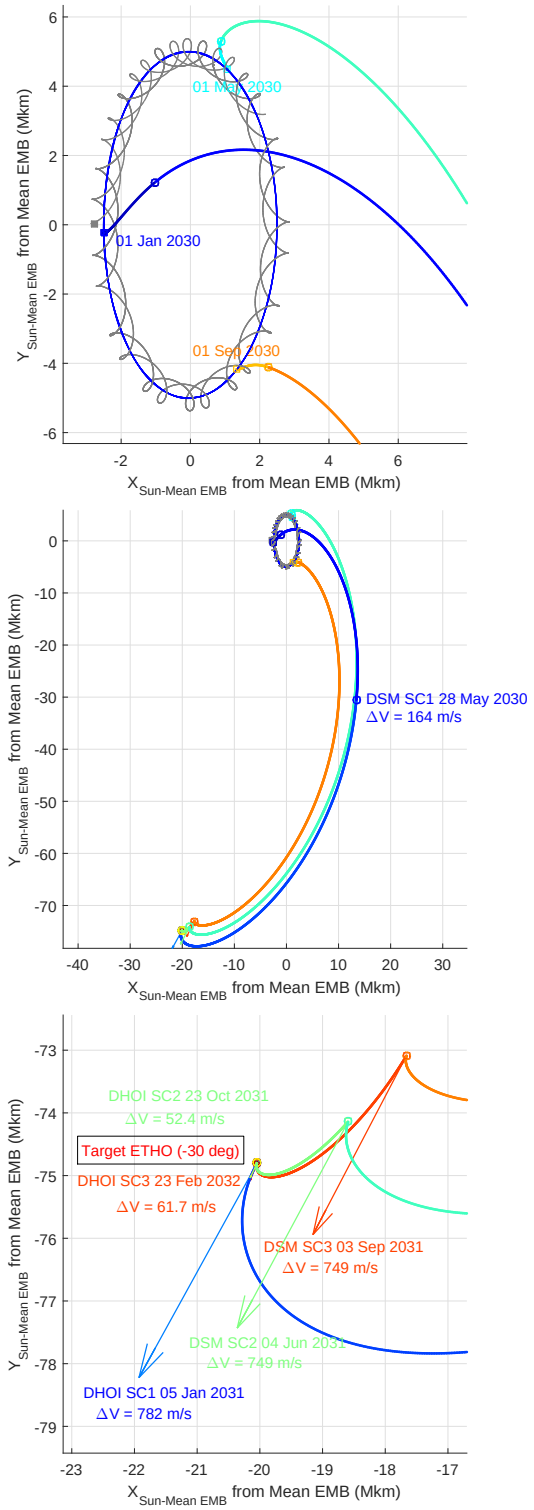

Fig. 12. Optimal heliocentric transfer trajectory examples for January (SC1), May (SC2) and September (SC3) launches. Injection, heliocentric transfer, and insertion trajectories and manoeuvres (arrows) are shown.

This comes at the expense of an increased transfer Delta-V depending on the launch month.

5. ALTERNATIVE TRANSFER STRATEGIES

In this section, alternative injection and transfer strategies are introduced and briefly discussed. While a direct ascent strategy leads to a simpler operational scenario and also represents the fastest available way to reach an EDHO, the motivations to investigate alternative options can be manifold, and some possible motives are listed below:

- Improve the mass efficiency of the transfer strategy, i.e. increase the mass delivered on the operational orbit,
- Ensure the compatibility with a lighter (lower cost) Launch Vehicle (LV),
- Ensure the compatibility with a dual launch scenario, with some constraints imposed by the other passenger spacecraft, potentially leading to a non-optimal injection orbit for the EDHO spacecraft.

5.1. Injection to LEO or HEO followed by Orbit Raising

The most straightforward alternative to the direct injection scenario by a Launch Vehicle is the case where the LV injects the spacecraft into an Earth-bound orbit, which then performs itself the trans-EDHO manoeuvre. Such a manoeuvre consists in an Apogee Raising Manoeuvre (ARM) performed at perigee, and can be either performed in a single manoeuvre, or in a multiple ARMs scenario, such as the one recently performed for the LEOP of the LISA Pathfinder (LPF) spacecraft [5]. A multiple ARMs strategy can be useful to reduce the gravity losses associated with any large manoeuvre, as well as to perform intermediary transfer orbit corrections. If starting from a Low Earth Orbit (either circular or elliptical like LPF), such an ARM sequence comes at a significant Delta-V cost. In order to increase the mass efficiency, this apogee raising can also be achieved by means of Electric Propulsion, in an Electric Orbit Raising (EOR) scenario. However, low-thrust EOR strategies lead to a significant increase of the LEOP duration and operational complexity.

5.2. Low Energy Escape via SEL1 or SEL2

A possible way to reduce the transfer Delta-V is to leverage the available orbital perturbations to raise (ETHO) or lower (ELHO) the *heliocentric* orbit semi-major axis. A proper orientation of the line of apses with respect to the Sun line will effectively raise the *geocentric* apogee up to escape. Such a transfer corresponds to a Weak Stability Boundary (WSB)-like transfer, escaping the Earth-Moon system via the unstable manifold of a Sun-Earth Lagrange Point Orbit (LPO). A large variety of solutions exist, only two examples will be shown to illustrate the strategy.

The first example considers a transfer to a -30 deg ETHO trailing orbit via SEL2[6], illustrated on Figure 13 and Figure 14. The scenario was optimised to minimize the total spacecraft Delta-V, assuming the (trans-L2) injection is performed by the Launch Vehicle. In this example the maximum date of the DSM was constrained to be 400 days (maximum) after injection, in order to avoid too long transfer solutions (see previous paragraph).

The osculating apogee altitude at injection is of about 1.3 Mkm, which needs to be compared to the injection V-infinity of 764 m/s in the direct injection scenario. The corresponding deterministic Delta-V saving (for the Launch Vehicle) is close to 55 m/s. Stochastic navigation manoeuvres for transfer corrections would also be slightly cheaper with this WSB transfer. However, more interestingly, the (DSM + HDOI) Delta-V for the spacecraft in this scenario is reduced down to about 811 m/s (compared to the previous 946 m/s), at the expense of an additional transfer duration of nearly 4 months. This Delta-V comes closer to the ideal Keplerian value (764 m/s) identified in the preliminary analysis, thanks to the better escape conditions geometry from the Earth-Moon system, enabled by the third-body perturbation of the Sun.

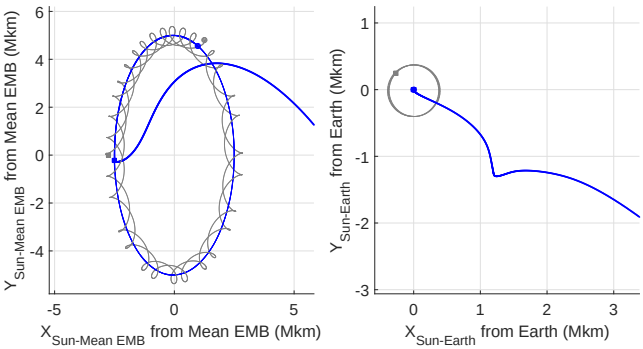

Fig. 13. Low energy escape via SEL2 in the Sun-MEMB (left) and Sun-Earth (right) rotating frames

It is also possible to escape via SEL1 to reach a trailing ETHO, but this is not optimal and would required again an additional transfer duration increase. Such a strategy could however be interesting in the case of dual launch scenarios where the orientation of the line of apses is constrained by one of the two spacecraft. In particular, dual launch Space Weather missions reaching SEL1 and SEL5 have been investigated, where the Launch Vehicle would inject the two spacecraft together on a trans-SEL1 trajectory. The objective is then to find suitable departure conditions from this transfer, using the unstable manifolds associated with the L1 orbit, to reach suitable escape conditions to reach SEL5.

For a Space Weather mission, the L1 spacecraft target orbit is likely to be a small or medium amplitude Lissajous

[6]Similar escape transfers to leading orbits can be achieved symmetrically via the inwards Sun-Earth Lagrange Point SEL1.

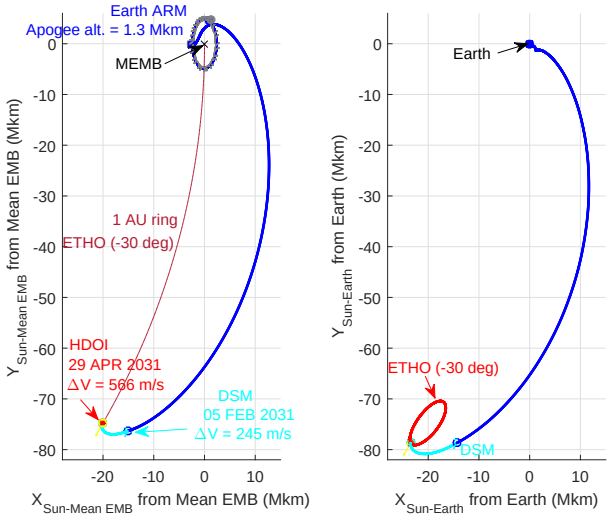

Fig. 14. Heliocentric transfer in the Sun-MEMB (left) and Sun-Earth (right) rotating frames

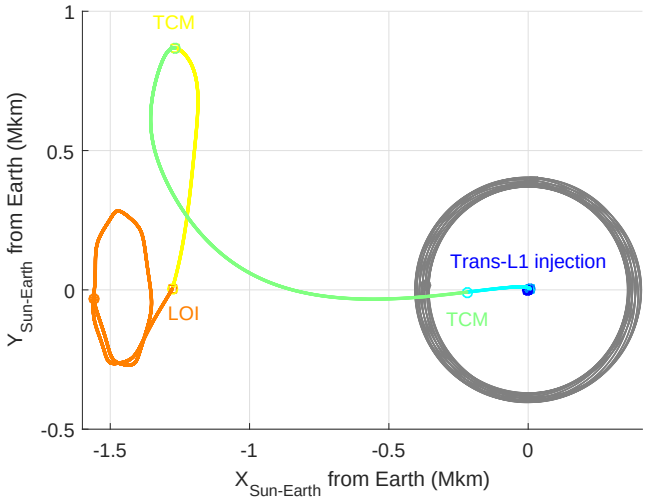

Fig. 15. DSCOVR transfer to SEL1 Lissajous Orbit

orbit, as opposed to a large orbit that could be reached via free injection transfer. Relevant examples of past missions are the Advanced Composition Explorer (ACE) and Deep Space Climate Observatory (DSCOVR) [6], which both targeted similar SEL1 orbits, An example is provided hereafter, using a trans-L1 transfer similar to the one performed by the DSCOVR spacecraft, as a study case. The DSCOVR injection scenario is characterised by the following sequence:

- Departure from a circular LEO at 185 km altitude, achieved by means of the Falcon 9 second stage ignition, and requiring about 3.2 km/s Delta-V,
- Two intermediate stochastic transfer correction manoeuvres are performed during the transfer (TCM),
- A LOI (Lissajous Orbit Insertion) is finally executed to reach the operational orbit, requiring a Delta-V of about 167 m/s.

A transfer similar to that of DSCOVR has been reproduced on Figure 15, in the Sun-Earth rotating frame.

In order to find suitable L5 transfers departing from this trajectory, a new optimisation is required, for which the optimisation parameters are the epoch, magnitude and direction of the departure manoeuvre (trans-L5 injection), in addition to the intermediate DSM and L5OI as in the direct injection transfer cases. The resulting transfer is presented on Figure 16, successively showing the injection, followed a small Delta-V manoeuvre (49 m/s) performed at the first apogee after 65 days, and a heteroclinic connection towards the SEL2 region. In this example, escape is achieved and SEL5 is reached after a two-revolution heliocentric transfer, leading to an overall transfer duration of about 3 years and a total Delta-V of 821 m/s (not accounting for the trans-SEL1 injection manoeuvre, assumed to be performed by the LV).

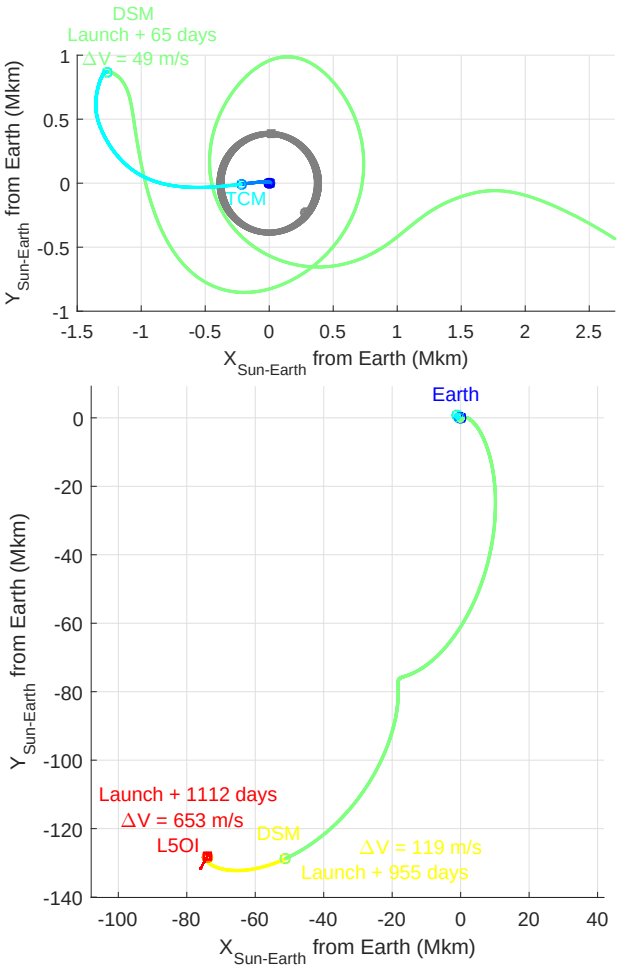

Fig. 16. Low energy escape via SEL1/SEL2 to SEL5 in the Sun-Earth (right) rotating frame

5.3. Use of Lunar Gravity Assists

In the previous section, the perturbation from the Sun's gravity was leveraged to raise the apogee of an Earth-bound orbit leading to a High Elliptical Orbit (HEO), eventually achieving escape conditions. It is possible to use an even lower High Earth Orbit (apogee) to reach the interplanetary transfer, by using another perturbation effect: the gravity of the Moon. In this section, the use of Lunar Gravity Assists (LGA) is discussed. Although being more complex operationally, LGA options can be very efficient to reach heliocentric orbits. Again, such strategies could be used either:

- For a single launch scenario, in order to increase the launcher performance by injecting into a negative C3 elliptical orbit, or a less energetic TLI (Trans-Lunar Injection) than would be required for direct escape.
- For dual launch scenarios, in order to modify the naturally optimal Local Solar Time of the ARM. The LGA could be performed by either one of the spacecraft, with the objective to reduce significantly the loitering time in Earth-bound orbit that would otherwise be potentially required for the other (waiting for the right alignment of the line of apses with respect to the Sun).

Like in the previous section, a large variety of solutions exist and a single sample LGA scenario, followed by a transfer to a -30 deg ETHO, will be illustrated in this section.

Even more in this LGA case, the assumptions regarding the Launch Vehicle play a critical role. In order to illustrate this, a launch with Ariane 6 from Kourou into GTO is assumed, followed by an Apogee Raising Manoeuvre targeting the Moon to perform the LGA. Because of the low inclination of the GTO orbit, as well as the assumption for the Argument of Perigee ($\omega = 178\,\mathrm{deg}$), the line of apses almost lies in equatorial plane, resulting in a reduced number of opportunities with reasonable Delta-V. These actually occur twice a month as the relative line of nodes geometry is favourable (Moon crossing the equator, either ascending or descending). Figure 17 shows an opportunity map, providing the TLI Delta-V required from a GTO orbit in January 2030. Only solutions with a departure Delta-V under 2 km/s are provided.

The opportunity map on Figure 17 shows a relatively low sensitivity of the TLI Delta-V as a function of the transfer duration. However, the tuning of this duration can significantly impact the arrival conditions at the Moon, both in terms of hyerpbolic approach geometry (azimuth, elevation) and in terms of energy. Figure 18 shows for the same dates and durations the corresponding arrival V-infinity at the Moon, which will be leveraged to performed the LGA.

Upon reaching the Moon, the definition of an LGA scenario requires additional parameters: these include the altitude of the periselene, as well as the B-angle. All these parameters result in a wide range of Earth-Moon escape conditions that are achievable to optimise a transfer to an EDHO. On the other hand, there are only limited opportunities, as there will be a discrete set of Moon positions in Sun-Earth rotating frame (local solar time) at which the LGA can occur throughout the year. A sample end-to-end example is shown below, using a 5 days ascending Moon transfer in January 2030. The sequence is the following:

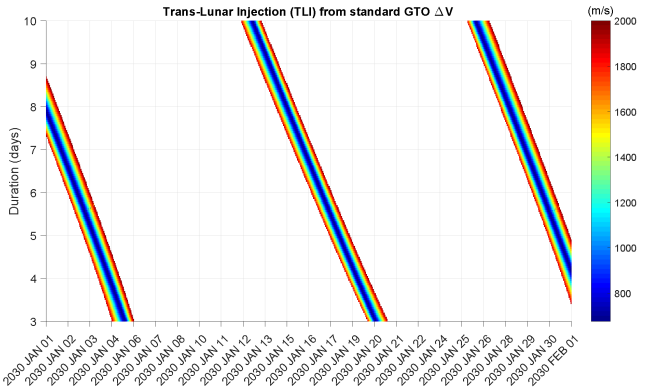

Fig. 17. TLI Delta-V from standard GTO in January 2030

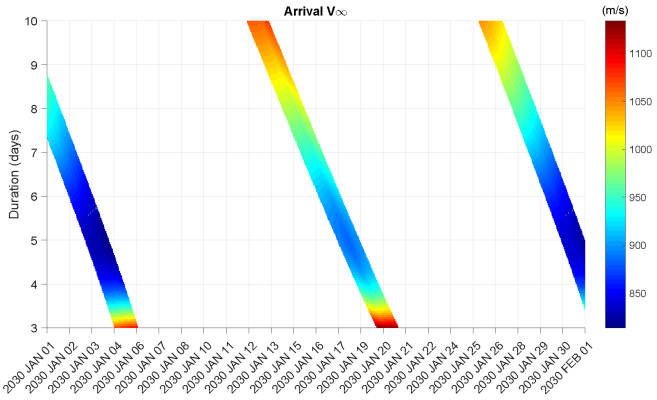

Fig. 18. Lunar arrival V-infinity

- TLI manoeuvre of 681 m/s from the GTO orbit, followed by a 5 days transfer to the Moon: the corresponding apogee altitude in that case is of only 386000 km,
- Lunar Gravity Assist on an ascending Moon, with a periselene altitude of about 510 km, leading to an escape of the Earth-Moon system,
- Deep Space Manoeuvre (40.8 m/s),
- HDOI (800.5 m/s) upon reaching the target ETHO.

The phases of the mission and transfer trajectory are illustrated on Figure 19 (injection, Lunar Gravity Assist and escape in Sun-Earth rotating frame) and Figure 20 (heliocentric transfer towards ETHO including DSM and HDOI). The first

figure shows how the LGA has permitted to drastically modify the initial orientation of the line of apses (pre-LGA) compared to the one that would be required for a direct injection transfer. This can be used for dual launch scenarios where this parameter is constrained by one or the other spacecraft.

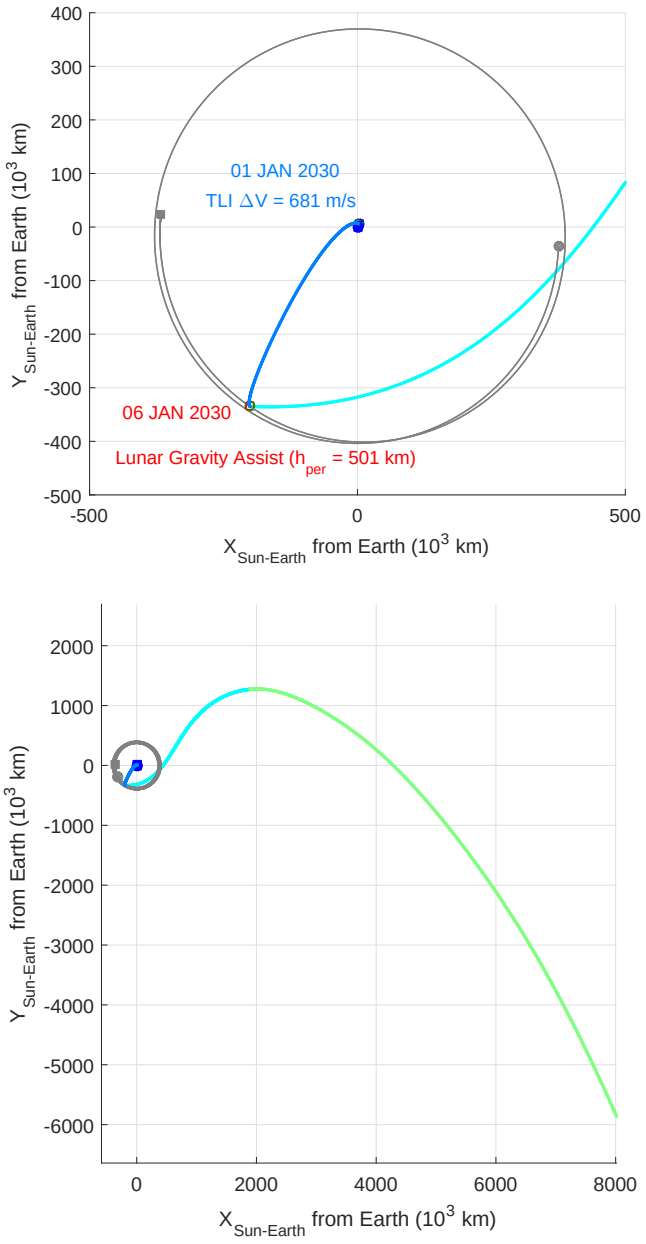

Fig. 19. Injection, LGA and escape in Sun-Earth rotating frame

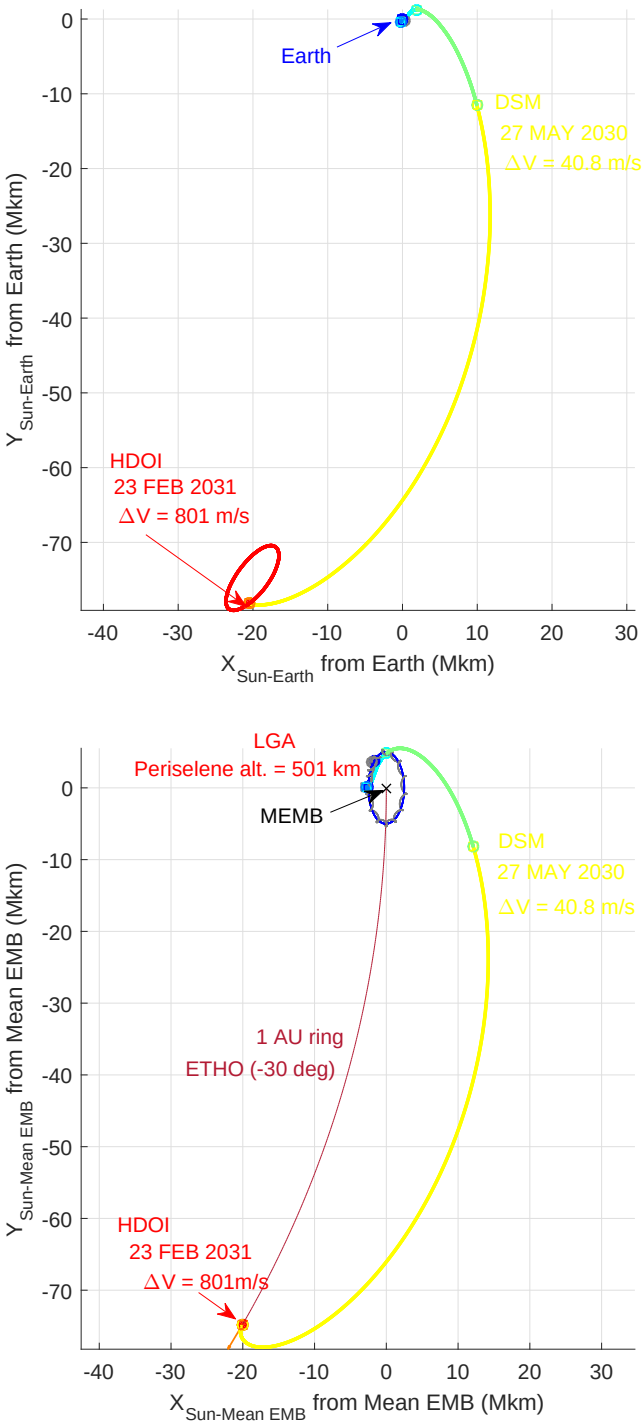

Fig. 20. Transfer in Sun-Earth rotating frame (middle), Sun-MEMB rotating frame (bottom)

On this example, the sum of the DSM and HDOI Delta-V amounts to 841.3 m/s, which is again significantly lower than the direct injection scenario. This value is close to that of the WSB transfer escaping via SEL2, but the transfer is two months shorter. Despite their increased operational complexity, LGA options are therefore powerful mission design tools, and their use has been demonstrated by the STEREO mission [1], which actually used two consecutive LGAs for STEREO-B to escape the Earth-Moon system towards its trailing drift-away operational orbit.

5.4. Transfers Augmented with Solar Electric Propulsion

The use of Solar Electric Propulsion (SEP) for interplanetary transfers can serve different purposes, depending on the mission. It is a useful way to reduce the Earth departure V-infinity (C3), thus increasing the available launch mass, and to perform the launch declination corrections that may be required with a lesser mass impact as compared to Chemical Propulsion (CP). It also provides the opportunity for a significant reduction of the propellant mass required for subsequent manoeuvres, thanks to the higher specific impulse (Isp) of the propulsion system. On the other hand, the design of SEP missions is made more complex by the strong interactions that exist between the spacecraft design and the transfer properties. SEP interplanetary transfers are also more challenging operationally than classical CP transfers: the concept of navigation and the associated performance of Orbit Determination (OD) have not been analysed in the context of the present study, but low-thrust transfer operations are likely to require some forced coast arcs for navigation and orbit correction, in particular prior to critical manoeuvres. In case of very low-thrust (the thrust-to-mass ratio is the key parameter), long thrust arcs are generally required for optimal transfers. Finally, for the spacecraft design itself, the cost and complexity of the actual EP thrusters need to be considered.

The examples provided consider again a mission launched in January 2030 towards a -30 deg ETHO. A thrust-to-mass ratio variation between 0.5 and 0.05 N/ton has been performed, in order to describe the evolution of the transfer properties when this parameter is varied. Table 2 provides the main results, in terms of SEP transfer Delta-V.In these examples, the same launch V-infinity as in the previous section has been assumed (764 m/s), in order to facilitate comparisons.

Table 2. SEP transfer results for January 2030 launch

Thrust-to-mass ratio (N/ton)	Delta-V (m/s)	Arrival date	Duration (days)
∞ (CP)	945.95	05/01/2031	369
0.5	949.77	14/01/2031	378
0.25	956.48	25/01/2031	389
0.125	1001.94	18/02/2031	413
0.0625	1141.12	26/03/2031	449
0.05	1325.73	04/05/2031	488

As evidenced by Table 2, the impact of a reduced thrust-to-mass ratio is to increase the required Delta-V as well as the transfer duration. There is in fact a limit under which the exponential increase in duration and Delta-V becomes prohibitive, also saturating the interplanetary arcs with thrust. Figure 21 and Figure 22 illustrate the transfer trajectory for the lowest thrust-to-mass ratio considered in this example, both in the Sun-MEMB rotating frame (top and middle), and in the ecliptic inertial frame (bottom).

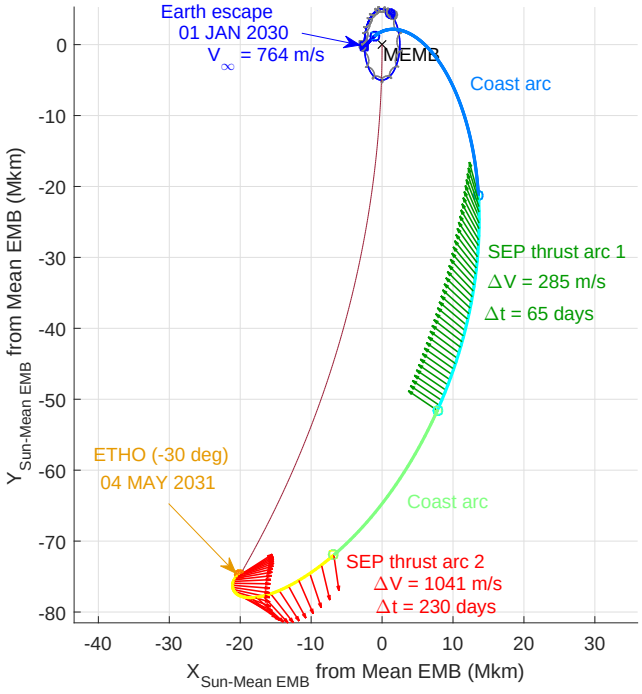

Fig. 21. Sample SEP transfer to -30 deg ETHO departing in January 2030 (Sun-MEMB rotating frame)

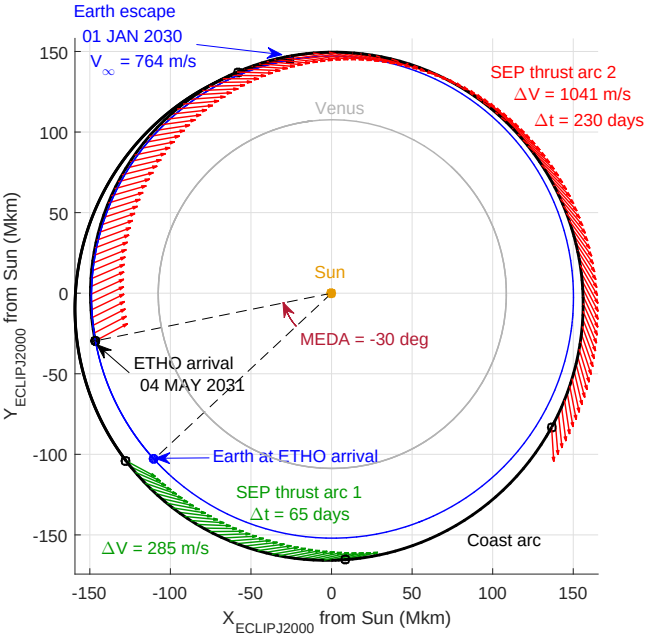

Fig. 22. Sample SEP transfer to -30 deg ETHO departing in January 2030 (inertial ecliptic frame)

6. CONCLUSION

This paper has reviewed several transfer strategies to reach Earth-Leading or Earth-Trailing Heliocentric Orbits, as candidate orbits for future operational or science missions. A new frame (the Sun-Mean Earth Moon Barycentre rotating frame) has been introduced as a convenient way to describe transfer trajectories to such target destinations, and the seasonal variations of the required transfer Delta-V have been described for a direct injection scenario into heliocentric transfer orbit. Several alternative strategies have been shown to be available, providing some flexibility in the optimisation of a mission architecture. While the direct injection transfers are both the fastest and the simplest options, other techniques can be used to reduce the load on the Launch Vehicle, and/or the propellant mass for the spacecraft, resulting in more mass efficient solutions. These include in particular low energy escape via the Sun-Earth Lagrange Points, as well as Lunar Gravity Assists. However, these alternative options come at the expense of an additional LEOP and/or transfer duration, as well as an increased operational complexity.

7. REFERENCES

[1] D.W. Dunham, J.J. Guzman, and P.J. Sharer, "Stereo trajectory and maneuver design.," *Johns Hopkins APL Technical Digest*, vol. 28, no. 2, pp. 104 – 125, 2009.

[2] J.H. Kwok, M.D. Garcia, E. Bonfiglio, and S.M. Long, "Spitzer space telescope mission design.," in *Proceedings of the SPIE - The International Society for Optical Engineering*, Jet Propulsion Lab., California Inst. of Technol., Pasadena, CA, USA, 2004, vol. 5487, pp. 201 – 210.

[3] K Arai, E. D Hall, S Vass, M Vallisneri, C Cahillane, W. Z Korth, R. W. P Drever, M. P Thirugnanasambandam, L. R Price, J. G Rollins, E. J Sanchez, J. C Barayoga, M. E Zucker, P Schmidt, T Callister, R. D Williams, A Singer, R Abbott, C. I Torrie, G McIntyre, G Billingsley, R Bork, M Pedraza, N. D Smith, S. B Anderson, N. A Robertson, J Zweizig, Y Chen, A. J Weinstein, G Vajente, V Kondrashov, R. J. E Smith, P. A Willems, W Kells, R. X Adhikari, J Heefner, T Etzel, M. B Jacobson, A Perreca, Z Shao, J. B Kanner, J. N Marx, Yamamoto H., B. P Abbott, R Chakraborty, E Maros, G. H Sanders, M Isi, T Chalermsongsak, S Meshkov, W Engels, C. B Cepeda, S.E Whitcomb, K. A Hodge, B. C Barish, M.R Smith, P Couvares, J. K Blackburn, J McIver, E. A Quintero, and Gossa, "Observation of gravitational waves from a binary black hole merger.," 2016.

[4] Collaboration The LIGO Scientific and Collaboration The Virgo, "Gw170817: Observation of gravitational waves from a binary neutron star inspiral.," 2017.

[5] A. Rudolph, I. Harrison, F. Renk, D. Firre, F. Delhaise, C.G. Marirrodriga, P. McNamara, B. Johlander, M. Caleno, J. Grzymisch, F. Cordero, D. Wealthy, and J.P. Olive, "Lisa pathfinder mission operations concept and launch and early orbit phase - in-orbit experience.," European Space Agency (ESA), European Space Operations Centre (ESOC), Robert Bosch Str 5, Darmstadt, 64293, Germany, 2016.

[6] Craig Roberts, Sara Case, Johnm Reagoso, and Cassandra Webster, "Early mission maneuver operations for the deep space climate observatory sun-earth l1 libration point mission," *AIAA/AAS Astrodynamics Specialist Conference ; 9-13 Aug. 2015; Vail, CO; United States*, 2015.